European Journal of Medicinal Chemistry 64 (2013) 160–168

Contents lists available at SciVerse ScienceDirect

European Journal of Medicinal Chemistry

journal homepage: http://www.elsevier.com/locate/ejmech

Original article

Elucidation of the pharmacophore of echinocystic acid, a new lead for blocking HCV entry

Han Wang [a,1], Qi Wang [a,1], Su-Long Xiao [a,1], Fei Yu [a], Min Ye [a,**], Yong-Xiang Zheng [a], Chuan-Ke Zhao [a], Di-An Sun [b], Li-He Zhang [a], De-Min Zhou [a,*]

[a] State Key Laboratory of Natural and Biomimetic Drugs, School of Pharmaceutical Sciences, Peking University, 38 Xueyuan Road, Beijing 100191, China
[b] Institute of Medicinal Plant Development, Chinese Academy of Medical Sciences and Peking Union Medical College, Beijing 100094, China

ARTICLE INFO

Article history:
Received 1 December 2012
Received in revised form
18 March 2013
Accepted 22 March 2013
Available online 3 April 2013

Keywords:
Echinocystic acid
Microbial transformation
HCV entry inhibitor

ABSTRACT

To elucidate the pharmacophore of echinocystic acid (EA), an oleanane-type triterpene displaying substantial inhibitory activity on HCV entry, two microbial strains, *Rhizopus chinensis* CICC 3043 and *Alternaria alternata* AS 3.4578, were utilized to modify the chemical structure of EA. Eight new metabolites with regio- and stereo-selective introduction of hydroxyl and lactone groups at various inert carbon positions were obtained. The anti-HCV entry activity of the metabolites **2**–**13**, along with their parental compound EA and other analogs **14**–**15**, were evaluated. Most of the metabolites showed no improvement but detrimental effect on potency except compound **5** and **6**, which showed similar and even a litter higher anti-HCV entry activity than that of EA. The results demonstrated that ring A, B, C and the left side of ring E of EA are highly conserved, while ring D and the right side of ring E of EA are flexible. Introduction of a hydroxyl group at C-16 enhanced the triterpene potency. Further analysis indicated that the hemolytic effect of EA disappeared upon such modifications.

1. Introduction

Pentacyclic triterpenes, mainly including lupane, oleanane, and ursane types [1,2], are secondary plant metabolites found in different plants, with a few species containing up to 30% of their dry weight [3,4]. It has been proposed that triterpenes possess defense activities and thus protect hosts from various pathogen and herbivore infections [5,6]. Betulinic acid, a lupane-type triterpene, has been shown by many studies to display significant inhibiting activity against HIV entry and maturation. One of its derivatives, bevirimat, is currently in clinical trials [7–9]. Moronic acid and hawthorn acid, two oleanane-type triterpenes, have also shown anti-HIV activity with even better antiviral profiles *in vitro* than bevirimat [10]. The diverse and promising biological activities of triterpenes, including anti-inflammatory [11,12], hepatoprotective [13], analgesic, antimicrobial, antimycotic, virostatic, immunomodulatory and tonic effects [14,15], warrant further investigation of their potential pharmaceutical uses.

Hepatitis C virus (HCV) infection is the leading cause of liver fibrosis and cirrhosis which eventually leads to liver cancer. Treatment of HCV infection has relied on ribavirin and interferon for almost 30 years with recently approved telaprevir and boceprevir representing the beginning of a new era targeting HCV replication [16]. However, resistance to antiviral drugs is likely to develop and combination of drugs targeting different stages of HCV viral life cycle is eventually required. Inhibition of viral entry into HCV-permissive cells represents an emerging field for reduction or elimination of productive infection. HCV entry inhibitors could satisfy the tandem mechanism for use with other inhibitors of viral replication, ultimately leading to a multifaceted approach to the eradication of HCV infection.

Recently, we found echinocystic acid (EA, compound **1** in Fig. 1), an oleanane-type triterpene, displayed substantial inhibitory activity on HCV entry with one derivative showing IC_{50} at sub-μM level. Although the mechanism underlying the blocking of HCV entry by EA is only narrowly understood, our recent study established the importance of triterpenes serving as parent compounds from which further potential entry inhibitors could be developed (manuscript in preparation). Aimed at rational design of specific inhibitors for viral entry, efforts are made to further elucidate the relationship between their structures and activities, and to define specific factors necessary for regulation of virus/host cell recognition. However, expansion of triterpene structural diversity via

* Corresponding author. Tel./fax: +86 10 8280 5519.
** Corresponding author. Tel.: +86 10 82802024.
E-mail addresses: yemin@bjmu.edu.cn (M. Ye), deminzhou@bjmu.edu.cn (D.-M. Zhou).
[1] Those authors have contributed equally to this work.

0223-5234/$ – see front matter © 2013 Elsevier Masson SAS. All rights reserved.
http://dx.doi.org/10.1016/j.ejmech.2013.03.041

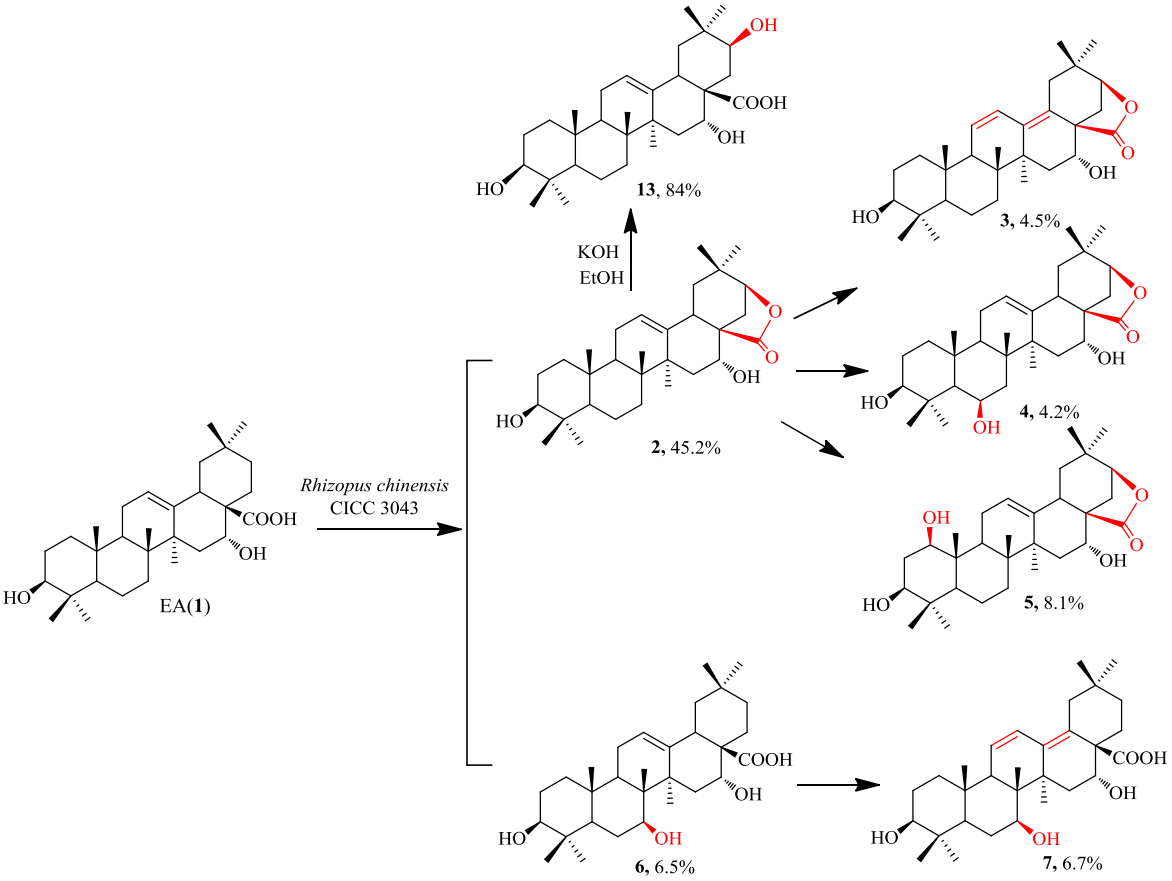

Fig. 1. The proposed route for *R. chinensis*–mediated biotransformation of EA.

chemistry approaches is limited because of the few chemical active sites within their skeletons. Here, we report a microbial transformation strategy to allow the regio- and stereo-selective introduction of hydroxyl, ketone and other groups at proper positions of EA, which are usually difficult to achieve by chemical means. Through such chemical expansion, ring A and B are confirmed as highly conserved pharmacophore for blocking HCV entry and ring D is flexible with introducing a hydroxyl group at C-16 significantly enhancing the potency of triterpene. More importantly, ring E was excluded as a potential modifiable site for improving potency.

2. Results and discussion

2.1. Screening of microorganisms

We carried out a preliminary screening to identify which microorganisms among 13 microbial strains that were widely used in our lab for biotransformation of steroids [17,18] and tetracyclic triterpenoids [19] were able to transform EA. We found strain *Rhizopus chinensis* CICC 3043 and *Alternaria alternata* AS 3.4578, rarely used for fermentations of triterpenes, consumed substrate EA within one week. After scale-up, 6 and 7 metabolites were generated respectively, with a total of 8 new compounds.

The major product from *R. chinensis* CICC 3043-mediated biotransformation was identified as metabolite **2** (45.2%), along with minor metabolites: compound **3** (4.5%), **4** (4.2%), **5** (8.1%), **6** (6.5%), and **7** (6.7%). Based on the structures of those metabolites, we proposed that the main modification by *R. chinensis* CICC 3043 on EA was initially directed to C-21, yielding metabolite **2**, which was then transformed into **3**, **4** and **5** simultaneously in almost the same yields (Fig. 1). Alternative metabolism pathway by *R. chinensis* CICC 3043 directed to C-7, yielding metabolite **6**, which was then dehydrated to form metabolite **7** (Fig. 1).

The major product by *A. alternata* AS 3.4578-mediated biotransformation was identified as metabolite **12** (20.0%) and **11** (10.0%), along with minor metabolites: compound **5** (9.1%), **7** (0.8%), **8** (7.3%), **9** (2.6%), and **10** (3.1%). Based on the structures of those metabolites, we proposed that the main modification by *A. alternata* AS 3.4578 on EA was initially directed to C-1, yielding metabolite **8**, which was then transformed into **5** and **11** simultaneously in almost the same yields. Alternative metabolite pathway by *A. alternata* AS 3.4578 directed to C-29, yielding metabolite **9**, which was then oxidized to metabolite **12**. Incubation of EA with *A. alternata* AS 3.4578 may also provide metabolite **7** and **10** (Fig. 2).

2.2. Structure elucidation of the metabolites

All the ^{1}H and ^{13}C NMR data of the new compounds **4**–**9**, **11** and **12** are given in Table 1 and Table 2, respectively.

Metabolite **2** was obtained as white powder, and was identified as the known compound acacic acid lactone, based on the strong absorption signal at 1763 cm^{-1} (the diagnostic IR feature for lactone) and the identical ^{1}H and ^{13}C NMR spectra as previously reported [20,21]. The change of the olefin chemical shift at δ_H 5.42 (H-12 of **2**) to δ_H 6.38 (dd, J = 10.5, 2.6 Hz) and δ_H 5.72 (d, J = 10.0 Hz), together with an identical γ-lactone IR absorption. The structure of metabolite **3** was further confirmed by comparison of ^{1}H and ^{13}C NMR spectra with those reported in the literature [22].

Metabolite **4** was isolated as colorless powder. The HR-ESI-MS showed an $[M + K]^+$ ion at m/z 525.2981 (calcd for $C_{30}H_{46}O_5K$,

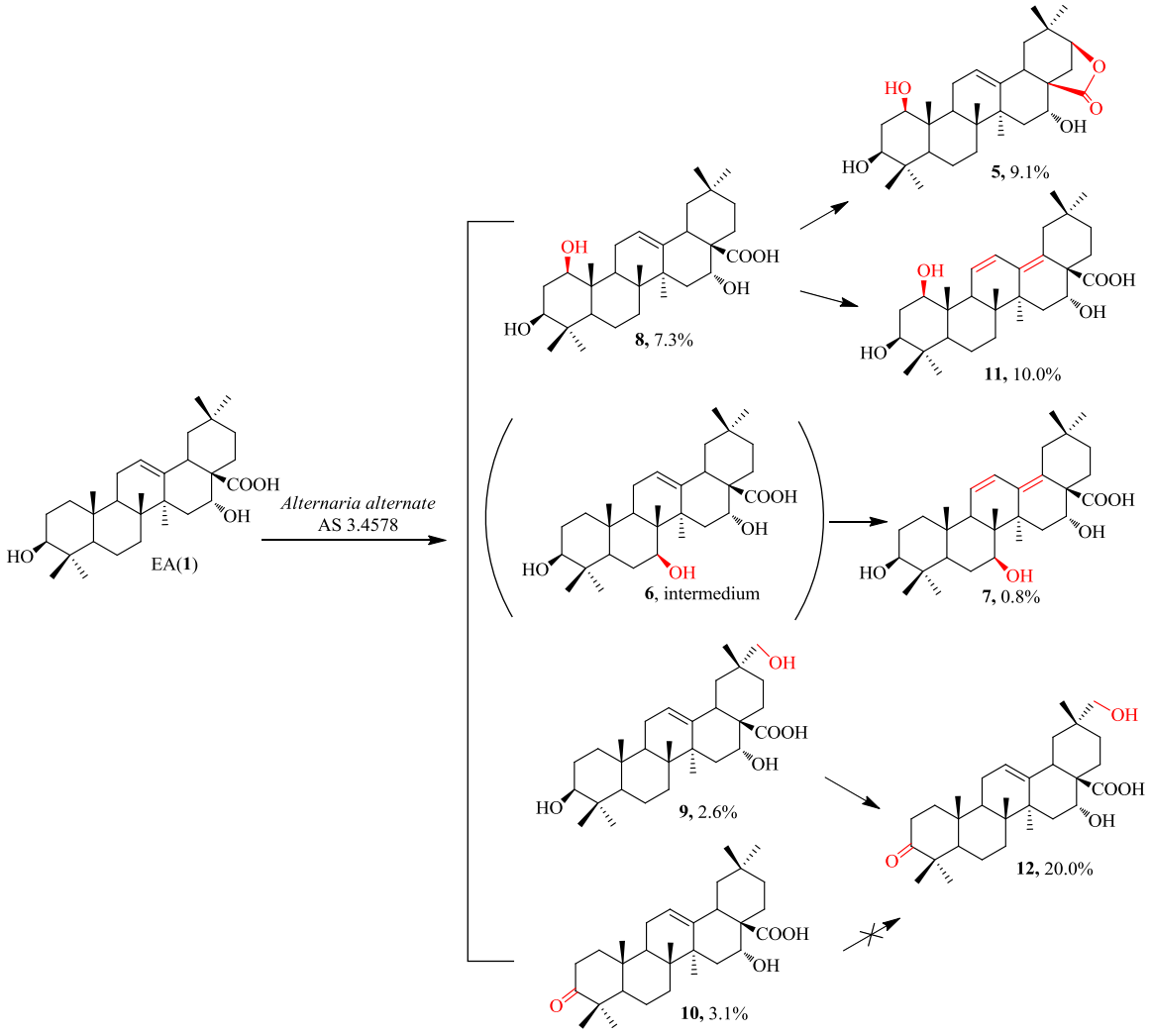

Fig. 2. The proposed route for *A. alternata*–mediated biotransformation of EA.

525.2977), together with a γ-lactone IR absorption at 1755 cm^{-1}, indicating it was a hydroxylated derivative of metabolite **2**. The ^{13}C NMR spectrum exhibited a new signal at δ_C 75.15 ppm rather than the original δ_C 19.66 ppm, a methylene attributed to C-6 in **2**, suggesting hydroxylation occurred at this position. Such deduction was consistent with the three–bond correlation between δ_H 0.99 ppm (collective signals for 23-, 30- and 24-CH_3) and δ_C 75.15 ppm observed in the HMBC spectrum (Fig. 3). The relative stereochemistry was established as 6β-OH based on NOESY spectrum which showed NOE enhancements between δ_H 1.32 (27-CH_3), δ_H 0.86 (H-5) and δ_H 3.86 (H-6).

Compound **5** was obtained as white powder with its molecular formula identified as $C_{30}H_{46}O_5$ based on its HR-ESI-MS. It also showed a lactone IR signal at 1766 cm^{-1}, suggesting it was a hydroxylated derivative of lactone (**2**). The new oxygen-bearing methine carbon at δ_C 80.21 correlated with a new proton at δ_H 3.33 (*m*) in the HSQC spectrum. However, the *W-type* long-range coupling of this new proton with H-3 (δ_H 3.17, m) was observed in the $^1H–^1H$ COSY spectrum (Fig. 3), together with the downfield shift of C-2 ($\Delta\delta$ 10.45 ppm) and the shift of δ_C 12.07 (C-25) supported a hydroxyl group introduced at C-1 position. The NOE correlations of H-1 with H-5 and H-3 indicated that the introduced hydroxyl group was β-oriented.

Metabolite **6** was isolated as white powder. The HR-ESI-MS showed an $[M + H]^+$ ion at *m/z* 489.3576, corresponding to the molecular formula of $C_{30}H_{48}O_5$, indicating a 16 amu mass increase comparing to that of **1**. The ^{13}C NMR and DEPT spectra exhibited a new signal at δ_C 74.42 ppm, which was correlated with a new proton signal at δ_H 3.85 ppm (1H, dd, J = 11.1, 4.8 Hz) in the HSQC spectrum. The HMBC spectrum disclosed long-range $^1H–^{13}C$ correlations of δ_H 3.85 with C-26 (δ_C 10.54) and C-14 (δ_C 44.13) and a correlation of δ_C 74.42 with C-26 methyl protons (δ_H 0.81) (Fig. 3). All these spectra supported hydroxylation occurred at C-7 position. The 7-OH was deduced to be β-oriented due to the observed NOE enhancement between δ_H 3.85 and 27-CH_3 (δ_H 1.43).

Metabolite **7** was obtained as white solid and was determined to have the molecular formula $C_{30}H_{46}O_5$ by HR-ESI-MS. There was a similar quarternary methyl group attached to an oxygenated carbon atom in the 1D NMR spectra of both **6** and **7**, suggesting β-hydroxylation of C-7. The NOE correlation between H-7 (δ_H 3.73) and 27-CH_3 (δ_H 1.30) confirmed the assignment that 7-OH was in β-orientation (Fig. 3).

Based on the structures of the metabolites in *A. alternata* AS 3.4578-mediated biotransformation, the initial metabolic products were compound **8** (7.3%), **9** (2.6%) and **10** (3.1%), supposedly produced simultaneously. The secondary metabolic products from **8** were compound **5** (9.1%) and **11** (10.0%) in almost the same yield. The secondary metabolic product from compound **9** was supposedly compound **12** (20.0%) (Fig. 2). It seemed that compound **10** was a final transformation product from the starting material. However,

Table 1
^{1}H NMR data (400 MHz in CD_3OD) of compounds **4**–**9**, **11** and **12**.

Position	4	5	6	7	8	9	11	12
1	0.86(m)	3.33(m)	1.72(m)	1.89(m)	3.34(m)	1.67(m)	3.45(m)	1.67(m)
				1.00(m)		1.07(m)		1.07(m)
2	1.63(m)	1.71(m)	1.58(m)	1.66(m)	1.92(m)	1.59(m)	1.78(m)	1.43(m)
3	3.15(m)	3.17(m)	3.15(dd; 11.0,9.1)	3.17(dd; 10.8,5.2)	3.17(dd; 9.0,7.7)	3.17(dd; 11.7,5.0)	3.19(m)	3.21 (m)
5	0.86(m)	0.62(m)	0.84(m)	0.84(m)	0.60(d; 8.4)	0.76(m)	0.64(d; 11.0)	0.84(m)
6	3.86(m)	1.65(m)	1.6(m); 1.50(m)	1.63(m)	1.58(m)	1.58(m)	1.58(m)	1.58(m)
7	1.32(m)	1.52(m)	3.85(dd; 11.1,4.8)	3.73(dd; 10.6,4.4)	1.51(m)	1.38(m)	1.73(m), 1.90(m)	1.41(m)
9	1.32(m)	3.30(m)	1.65(m)	1.90(m)	1.72(m)	1.67(m)	2.20(m)	1.82(m)
11	1.98(m)	2.50(m)	1.90(m)	6.49(d; 5.0)	2.44(m)	1.93(m)	6.37(d; 10.2)	1.93(m)
		2.13(m)			2.06(m)	0.99(m)		0.99(m)
12	5.47(s)	5.41(s)	5.34(s)	5.55(d; 10.6)	5.28(m)	5.34(m)	6.69(d; 11.0)	5.37(m)
15	1.64(m)	2.03(dd; 14.2,5.0)	2.07(m)	2.17(m)	1.84(m)	1.88(m)	1.38(m)	1.95(m)
		1.09(m)	1.82(d; 14.8)	1.77(m)	1.33(m)			
16	3.90(m)	3.90(dd; 11.7,4.9)	4.43(s)	4.11(s)	4.45(s)	4.47(s)	4.10(s)	4.47(m)
18	2.47(dd; 12.0,6.6)	2.48(m)	3.00(dd; 14.3,3.5)		2.98(dd; 14.3,4.2)	3.05(dd; 14.0,3.5)		3.07(dd; 14.3,4.1)
19	1.35(m)	1.82(m)	2.30(m)	1.87(m)	2.28(m)	2.27(m)	2.55(d; 14.6)	2.27(m)
		1.37(dd; 6.7,4.3)		2.56(d; 14.7)	1.00(m)	1.09(m)	1.81(m)	1.09(m)
21	4.24(d,5.4)	4.25(d; 5.5)	1.90(m); 1.15(m)	1.38(m)	1.72(m)	1.94(m)	1.38(m)	1.94(m)
22	1.23(m)	2.32(dd; 12.0,5.6)	1.90(m)	1.91(m)	1.89(m)	1.78(m)	2.08(m)	1.82(m)
		2.18(d; 11.9)	1.72(m)		1.78(m)	1.82(m)	1.92(m)	1.78(m)
23	0.99(s)	0.95(s)	0.83(s)	0.97(s)	0.94(s)	0.99(s)	0.93(s)	1.10(s)
24	0.99(s)	0.77(s)	0.77(s)	0.76(s)	0.75(s)	0.80(s)	0.74(s)	0.89(s)
25	0.95(s)	0.97(s)	0.94(s)	0.90(s)	0.96(s)	0.98(s)	0.97(s)	1.09(s)
26	0.79(s)	0.93(s)	0.81(s)	0.78(s)	0.79(s)	0.83(s)	0.77(s)	1.07(s)
27	1.32(s)	1.25(s)	1.43(s)	1.30(s)	1.37(s)	1.40(s)	0.83(s)	1.40(s)
29	1.01(s)	1.00(s)	0.88(s)	0.92(s)	0.87(s)	3.21(s)	0.92(s)	3.22(s)
30	0.99(s)	0.99(s)	0.95(s)	0.83(s)	0.96(s)	1.02(s)	1.25(s)	1.02(s)

it is not clear what pathway generated compound **7**. It is potentially from intermediate **6** which was detected at day 3 but not at day 7, during the time course of monitoring EA biotransformation (Fig. 4).

The molecular formula of metabolite **8**, a white powder, was assigned as $C_{30}H_{48}O_5$ based on its HR-ESI-MS at *m/z* 489.3577, a 16 mass unit increase over the starting material. The similar ^{1}H and ^{13}C NMR spectral data of ring A as that of **5**, and the COSY correlations of H-1 and H-3 supported a hydroxyl group was introduced at C-1 position. The NOE enhancements between H-1 (δ_H 3.34), H-3α (δ_H 3.17) and H-5α (δ_H 0.60) confirmed the hydroxyl group adopting β-orientation (Fig. 3).

Table 2
^{13}C NMR data (100 MHz in CD_3OD) of compounds **4**–**9**, **11** and **12**.

Position	4	5	6	7	8	9	11	12
1	30.29	80.21	39.80	39.10	80.60	39.91	80.67	40.62
2	27.91	38.34	27.94	27.77	38.34	27.89	38.47	35.07
3	79.35	76.72	79.46	79.46	76.87	79.70	76.83	220.56
4	39.60	44.20	39.60	39.12	41.15	39.84	42.51	47.33
5	54.21	54.68	54.06	53.98	54.69	56.89	53.78	56.55
6	75.15	19.09	30.53	30.52	19.16	19.50	18.92	20.24
7	39.97	33.40	74.42	74.04	34.38	34.26	33.43	33.69
8	45.24	41.78	46.41	39.67	42.48	40.67	43.02	40.32
9	48.49	49.17	48.32	54.18	48.95	48.20	55.83	48.47
10	38.58	39.86	38.26	37.70	39.85	38.16	39.97	38.23
11	24.58	28.08	24.53	127.00	28.07	24.46	125.67	24.54
12	126.31	126.98	123.69	126.37	124.55	123.65	131.89	123.46
13	140.45	139.56	144.74	137.00	143.98	144.87	137.44	144.95
14	46.35	44.29	44.13	43.68	44.29	42.63	43.70	42.45
15	39.62	38.02	39.53	36.54	36.28	36.21	37.61	36.61
16	67.86	67.94	75.44	71.43	75.33	75.04	71.41	74.96
17	50.64	50.72	49.64	48.20	49.55	50.08	54.39	50.10
18	43.31	42.61	42.84	131.24	41.94	41.30	129.37	41.38
19	43.60	44.01	47.76	41.68	47.69	42.47	41.40	42.78
20	34.95	34.86	31.40	32.81	31.40	36.60	32.79	36.19
21	85.25	85.19	36.57	37.54	36.60	31.35	37.61	37.90
22	27.61	27.49	32.36	29.57	32.28	31.30	29.45	31.29
23	28.64	28.56	28.66	28.33	28.61	28.74	28.40	27.10
24	16.42	16.00	16.38	15.71	16.01	16.33	15.55	21.87
25	16.13	12.07	16.01	18.80	11.97	16.03	14.88	15.68
26	10.82	16.93	10.54	12.41	18.06	17.77	17.54	17.63
27	29.16	29.19	27.24	22.06	27.18	27.32	24.96	27.25
28	183.22	183.11	181.16	179.94	181.16	181.05	180.00	180.98
29	28.93	28.96	33.41	32.90	33.43	74.83	32.92	74.80
30	24.35	24.26	24.91	24.99	24.88	20.25	21.47	20.75

The molecular formula of compound **9,** isolated as a white power, was $C_{30}H_{48}O_5$ based on HR-ESI-MS $[M + H]^+$ at *m/z* 489.3578. It was also a monohydroxylated metabolite of the starting material based on 16 amu mass increase. The disappearance of one methyl signal instead of an oxygenated methylene signals, δ_C 74.83 ppm and δ_H 3.21 ppm, plus the change of C-19, C-20 and C-21 chemical shifts in ^{1}H and ^{13}C NMR suggested the hydroxylation site was either at C-29 or C-30. The NOE correlation of methyl proton signal δ_H 1.02 (CH_3-30) with δ_H 3.05 (H-18), indicated the introduced hydroxyl group was located at C-29 (Fig. 3).

The less polar metabolite from *A. alternata* AS 3.4578-mediated biotransformation was **10**, which displayed a molecular formula of $C_{30}H_{47}O_4$ based on the HR-ESI-MS data. Comparison of its NMR data with that of **1** revealed that metabolite **10** is the previously reported 3-*oxo* derivative of echinocystic acid [23,24].

Metabolite **11** was also a white powder with molecular formula of $C_{30}H_{46}O_5$ based on $[M + H]^+$ at *m/z* 487.3412, the same as metabolite **7** but 2 amu mass less than **8**. The almost identical ^{13}C NMR spectra between metabolite **11** and **7** but an oxygenated quaternary carbon, δ_C 80.67 ppm versus δ_C 74.04 ppm, indicated their structure similarity. The HSQC correlation of this new oxygenated carbon with δ_H 3.45 ppm, which displayed a correlation with 25-CH_3 (δ_H 0.97 ppm) in HMBC and a *W*-type long-range coupling with H-3 (δ_H 3.19 ppm, *m*) in the ^{1}H–^{1}H COSY spectrum, demonstrated that C-1 was hydroxylated. The NOE correlations H-1 with H-3 and H-5 indicated its β-orientation (Fig. 3).

Compound **12** had a molecular formula of $C_{30}H_{46}O_5$ as determined by HR-ESI-MS ($[M + H]^+$ at *m/z* 487.3409), 2 amu mass less than that of metabolite **9**. The almost identical ^{1}H and ^{13}C NMR between compound **12** and **9**, together with the appearance of a carbonyl signal at δ_C 220.56 ppm but disappearance of a methine

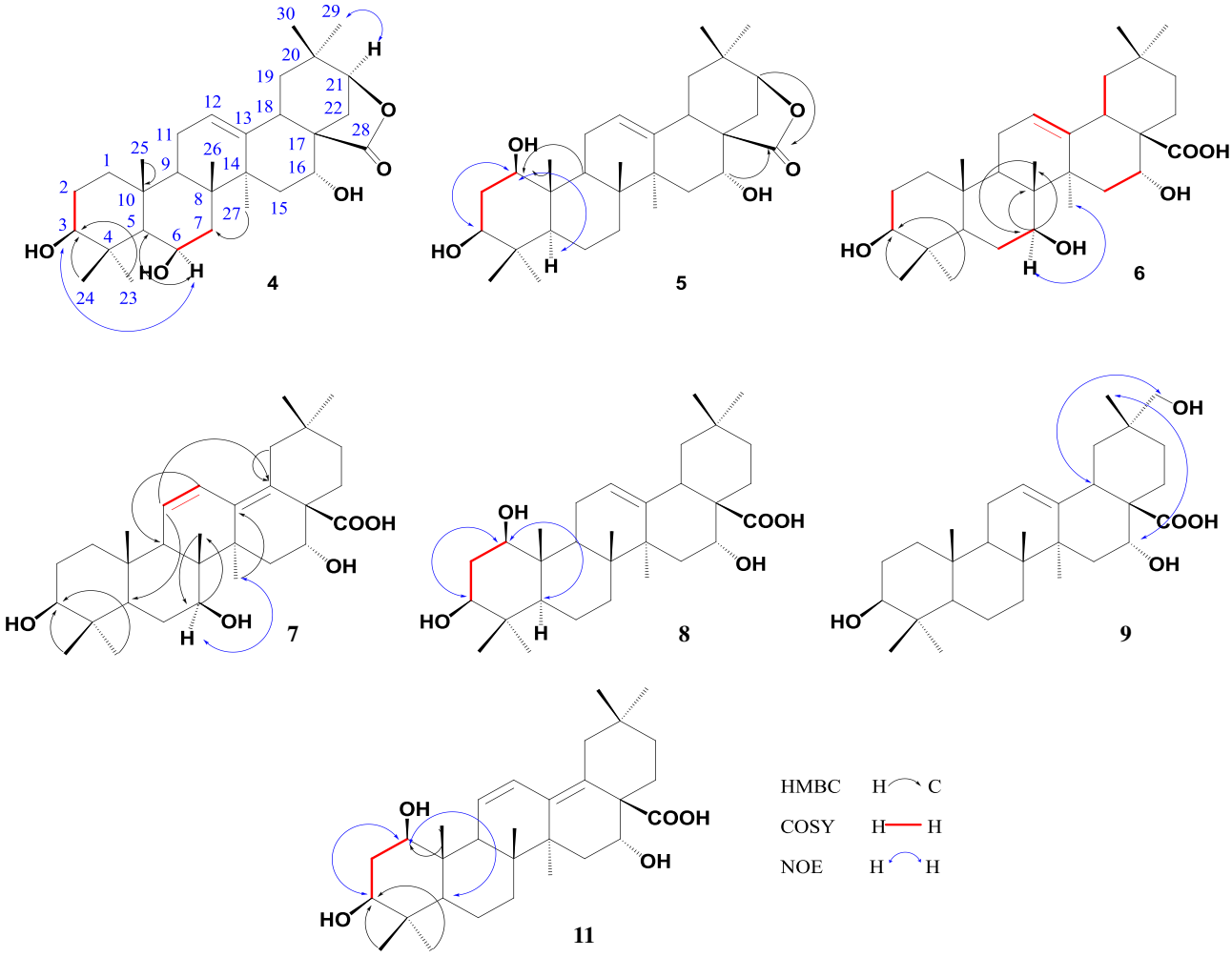

Fig. 3. Schematic representation of key HMBC, COSY and NOE correlations of EA metabolites **4**–**9** and **11**.

proton signal corresponding to C-3 (δ_H 3.17) suggested C-3 was a ketone, which was further supported by the downfield shifts of C-2 and C-4 by 7.01 and 7.26 ppm, respectively.

In order to test whether the isolated compounds are single isomers, enantiomeric mixtures or diastereomeric mixtures, we performed asymmetric HPLC analyses using a chiral column. As shown in Fig. R1 (Supporting information), all products were clearly separated with only one single peak detected for each of all products, suggesting all isolated products were optically pure with >95% purity. Combinations of the clear ^1H, ^{13}C NMR data and the asymmetric HPLC results excluded the possibility that the isolated products were enantiomeric or diastereomeric mixtures but single isomers.

2.3. Lactonization of EA by R. chinensis CICC 3043

One major feature observed in *R. chinensis* CICC 3043–mediated biotransformation was the formation of a lactone group in most of the metabolites. Such regio- and stereo-selective condensation of 21-CH_2 with 28-COOH is almost impossible by routine chemical means due to the inert characteristics of 21-CH_2. The lactone formation suggests the presence of a potential enzyme in *R. chinensis* CICC 3043 that displays strong capability for intramolecular esterification. Such enzyme, once identified, should have broad applications for diversity expansion of a variety of triterpenes. Lipase named RCL-lip2, isolated from *R. chinensis* CCTCC M201021, was found to catalyze the esterification of short-chain fatty acids [24]. It remained to be elucidated whether the same enzyme is responsible for formation of such lactones.

2.4. The effect of 16-hydorxyl group on biotransformation of triterpenes

Another remarkable observation in this study was the significant contribution of 16-hydroxyl that boosted the efficiency on biotransformation of triterpene. A 7-day fermentation of EA with *R. chinensis* CICC 3043 and *A. alternata* AS 3.4578 converted around 80% starting material into various metabolites. In contrast, a parallel fermentation of oleanolic acid (OA) by both fungi harvested nothing but the starting material. The molecular structure of EA is only slightly different from that of OA, –CHOH– versus –CH_2– at C-16. The poor biotransformation of OA is likely due to the lack of the hydroxyl group at C-16, which presumably activates the backbone of EA for introducing multiple hydroxyl groups at various positions. A reciprocal subjection of ursolic acid and betulinic acid, two lupane- and ursane-type triterpenes both lack of 16-OH, to the transformation by both fungi afforded nothing but the starting material, which also supported such conclusion.

2.5. The pharmacophore of EA for blocking HCV entry

We have demonstrated that triterpenoid natural products might serve as a distinct chemical class for the development of potent

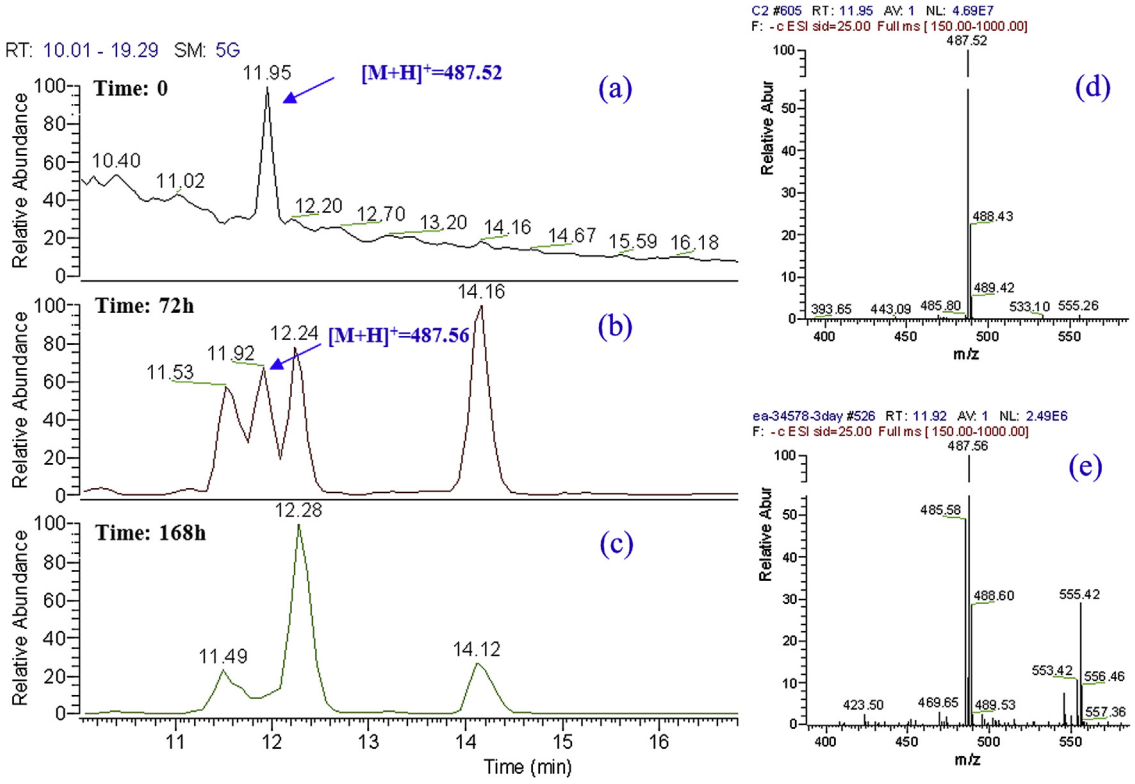

Fig. 4. LC-MS detected by *m/z* 486 profile of compound **4** (a) and compound **1**'s metabolites obtained from the extraction of the *A. alternata* culture medium at $t = 72$ h (b) and $t = 168$ h (c); mass spectrum of compound **4** giving *m/z* 487.53 $[M + H]^+$ (d); mass spectrum of peak B giving *m/z* 487.56 $[M + H]^+$ (e).

HCV entry inhibitors. Evaluation of EA analogs obtained in this study may help to clarify the triterpene SAR, in particularly, the pharmacophore of EA for blocking HCV entry. Initial SAR exploration at ring A and B, including hydroxylation at C-1 (**8**) or C-7 (**6**) and oxidation of C-3 (**10**), indicated all modifications significantly decreased the potency of EA (Table 3), confirming the previous observation that the left side of EA is conserved (Fig. 5). Modifications at the middle side of EA, such as dehydrations at ring C together with a hydroxyl group at either C-1 (**11**) or C-7 (**7**) or with a lactone between C-28 and C-21 (**3**), also significantly decreased the potency of EA (Table 3). This is also consistent with previous observations that chemical introduction of a hydroxyl (**14**) or a ketone (**15**) group at this region abolished the function of EA [25].

Table 3
Effect of metabolites **2**–**13** and compounds**14**–**15** on blocking HCV and VSV entry.

Compound	Anti-HCV (%)		Anti-VSV (%)	
	1 μM	5 μM	1 μM	5 μM
2	13.9 ± 2.1	31.9 ± 2.3	−17.3 ± 5.6	−12.1 ± 4.9
3	11.6 ± 1.7	31.7 ± 2.0	−16.2 ± 3.2	−10.3 ± 2.8
4	−1.0 ± 0.4	4.7 ± 0.9	−8.3 ± 2.6	−24.0 ± 3.0
5	28.9 ± 3.2	72.6 ± 2.8	1.8 ± 1.2	19.2 ± 1.7
6	30.4 ± 2.9	53.5 ± 3.1	1.6 ± 1.1	5.6 ± 1.9
7	22.2 ± 1.3	31.9 ± 1.9	−13.7 ± 2.0	−4.4 ± 1.9
8	14.3 ± 0.7	35.2 ± 1.2	7.9 ± 2.6	11.8 ± 2.1
9	16.5 ± 2.3	36.5 ± 1.7	−2.5 ± 0.9	3.6 ± 1.1
10	7.5 ± 1.3	41.6 ± 1.8	−2.5 ± 1.0	13.6 ± 1.5
11	2.3 ± 0.6	26.3 ± 0.8	−15.8 ± 2.3	5.9 ± 1.2
12	3.1 ± 0.0	−3.3 ± 0.7	−20.0 ± 3.7	10.7 ± 4.3
13	−5.7 ± 2.3	18.4 ± 1.8	20.7 ± 0.8	33.2 ± 0.6
14[a]	4.9 ± 0.3	−8.7 ± 0.7	42.7 ± 3.5	46.1 ± 4.1
15[a]	22.6 ± 1.9	51.0 ± 0.2	35.8 ± 1.5	43.5 ± 0.1
EA(1)	21.3 ± 2.1	75.5 ± 1.7	−0.1 ± 1.3	−0.1 ± 0.7

[a] Compounds **14** and **15** were semi-synthesized from EA [25].

Continuous exploration at ring D including hydroxylation at C-16 (EA versus OA) resulted in significant increase in potency (Table 3), suggesting ring D of oleanane-type triterpene is tolerant to modification and introduction of proper groups other than hydroxyl may further enhance its potency (Fig. 5). However, modifications at ring E, including hydroxylation at C-29 (**9**) and lactonization of C-28 with C-21 (**2**), reduced EA potency by over 50%. Further modifications of metabolite **2**, the hydroxylation at C-1 (**5**) and C-6 (**4**), showed the similar or even a little higher anti-HCV entry activities. However, dehydration at C-11 and C-12 and hydrolysis of the lactone (**13** and acacic acid lactone [26–28]) showed no improvement but detrimental effect on potency (Table 3). All data excluded ring E modification, but ring D was a potential modifiable site for further chemical modification (Fig. 5). This result led us to focus efforts on chemical optimization of ring D for improving the potency of EA. One derivative showed IC_{50} at 10 nM for blocking HCV entry [25].

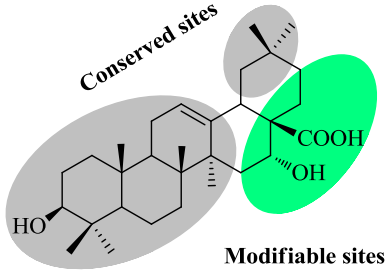

Fig. 5. Schematic representation of the conserved and modifiable sites within oleanane-type triterpenes for blocking HCV entry.

2.6. Depletion of the hemolytic effect of EA

A series of studies have demonstrated that the aglycons of triterpenoids play an essential role in the hemolytic properties [29–31], one of the well known characteristics of saponins. Compared with OA which possesses mild hemolytic activity, EA which gains a hydroxyl group at C-16, showed substantial hemolytic effect with CC_{50} at 15 μM (Fig. 6). Such hemolytic property, once enhanced in those afforded triterpene metabolites, may restrict their pharmaceutical use as potential anti-HCV entry inhibitors. Here, we found that hydroxylation of EA at C-1 (**8**), C-7 (**6**), C-29 (**9**), oxidation of C-3 (**10**) and lactonization of C-28 (**2**) depleted the hemolytic property (Fig. 6). Further modifications of those compounds with formation of lactones (**4** and **5**) or dehydration (**3**) did not increase their hemolytic effect (Fig. 6). It is possible that the biotransformation depletes the intrinsic hemolytic property of EA, which deserves further exploration.

3. Conclusion

In summary, we have expanded the structural diversity of EA via biotransformation and elucidated its pharmacophore that is needed for blocking HCV entry. We found most of the metabolites showed no improvement but detrimental effect on the potency except compound **5** and **6**, which showed similar and even a litter higher anti-HCV entry activity than that of EA. We concluded that ring A, B, C and the left side of ring E of EA are highly conserved, while ring D and the right side of ring E of EA, including C-28, are flexible. Introduction of proper groups at proper positions may enhance the potency of triterpenes. In addition, the substantial hemolytic property of EA disappeared upon such bio-modifications.

4. Experimental

4.1. Chemistry-general

Melting points were determined with an X-4 apparatus and uncorrected. Optical rotations were measured with a Rudolph Autopol III polarimeter. UV spectra were detected with a TU-1901 UV–Vis spectrophotometer. IR spectra were recorded in KBr with a NEXUS-470 FT-IR spectrophotometer. ^1H and ^{13}C NMR spectra were recorded in CD_3OD on Bruker Avance III spectrometer operating at 400 and 100 MHz. High Resolution Mass Spectra (HRMS) were obtained on an APEX IV FT_MS (7.0 T) spectrometer (Bruker) in positive ESI mode. Reversed-phase preparative HPLC was performed on an Alltech 426 HPLC system, using an Agilent Zorbax SB C_{18} chromatographic column (5 μm, 9.4 mm × 250 mm) with UV detection at 215 nm and RI 2000 detector. In order to confirm whether the synthesized compounds are single isomers, enantiomeric mixtures or diastereomeric mixtures, we further performed HPLC using Agilent 1100 HPLC system and Shiseido Capcell Pak Chiral CD-Ph C18 chromatographic column (5 μm, 4.6 mm × 250 mm) (Shiseido Co., Ltd., Tokyo, Japan), which frequently utilized in the enantiomeric impurity determination [32,33], under UV 215 nm. Mobile phase was acetonitrile (A) and water (B) with gradient as: 0–25 min, 20–60% A; 25–40 min, 60–90% A; 40–45 min, 90% A, and flow rate at 1.0 mL/min.

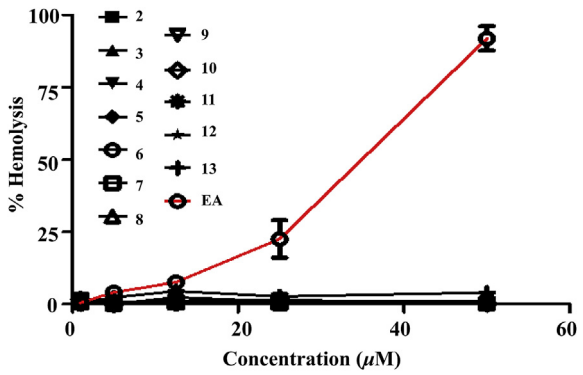

Fig. 6. Hemolytic properties of EA metabolites.

Column chromatography was performed on silica gel (200–300 mesh, Qingdao Haiyang Chemical Co. Ltd, China), and Sephadex LH-20 (Pharmacia Biotech AB, Sweden). Fractions were monitored by TLC, and spots were visualized by spraying the plate with 10% H_2SO_4 solution in EtOH followed by heating at 110 °C. All reagents and solvents were of analytical grade.

4.2. Microorganisms and culture media

The substrate EA was isolated from *Gleditsia japonica* and *Gymnocladus chinensis* [34]. A total of 13 different fungal strains, including *Alternaria alternata* AS 3.4578, *Doratomyces stemonitis* AS 3.1411, *Fusarium avenaceum* AS 3.4594, *Mucor spinosus* AS 3.3450, *R. chinensis* CICC 3043, *Syncephalastrum racemosum* AS 3.264, *Cunninghamella elegans* AS 3.1207, *Chaetomium globosum* IFFI 2445, *Crebrothecium ashbyii* ACCC 2114, *Absidia coerulea* AS 3.3389, *Aspergillus niger* AS 3.795, *Gibberella fujikuroi* var. *fujikuroi* AS 3.4748, *Saccharomyces cerevisiae* ACCC 2168, were screened in the preliminary test for their capabilities to metabolize EA. All fungal strains were purchased from China General Microbiological Culture Collection Center (CGMCCC) or China Center of Industrial Culture Collection (CCICC). All of the microorganisms were freshly subcultured prior to the biotransformation experiments. All preliminary screening experiments were performed by a two-stage fermentation procedure in potato media.

Fermentations were carried out in potato media consisting of 20 g of potato extract (prepared from 200 g of potato slices extracted in boiling water for 30 min), 20 g of glucose, and 1000 mL of water. The media were sterilized at 121 °C and 1.06 kg/cm^2 for 20 min. The strains were maintained on potato dextrose-agar (PDA) medium slants and stored at 4 °C.

4.3. Biotransformation of EA by R. chinensis CICC 3043

Mycelia of *R. chinensis* CICC 3043 from agar slants were aseptically transferred to 1000 mL Erlenmeyer flasks containing 400 mL of liquid potato medium. The fungus was incubated at 25 °C on a rotary shaker (180 rpm). After 48 h incubation, a total amount of 900 mg of EA dissolved in 50 mL of EtOH was distributed equally among 50 flasks. The incubation was allowed to continue for seven additional days on the shaker. The cultures were then pooled and filtered through a filter paper. The filtrate was extracted with equal volume of EtOAc for three times. The organic layer was dried over anhydrous Na_2SO_4, filtered, and evaporated *in vacuo* to afford a brown syrup. The syrup was subjected to column chromatography on silica gel using petroleum ether/EtOAc (98:2 to 0:100, v/v) as eluting system to afford fifteen fractions, followed by a purification step on a Sephadex LH-20 column. Fr. 3–5 was subjected to preparative HPLC and eluted with CH_3CN–H_2O (50:50, v/v) to give **2** (76.5 mg). Fr. 8–10 was purified by preparative HPLC and eluted with CH_3CN–H_2O (50:50, v/v) to give **6** (39.4 mg). Fr. 11 was subjected to preparative HPLC and eluted with CH_3CN–H_2O (50:50, v/v) to give **5** (50.4 mg). Fr. 12–14 was subjected to preparative HPLC and eluted with CH_3CN–H_2O (45:55, v/v) to give **4** (21.6 mg). Fr. 15 was subjected to preparative HPLC and eluted with CH_3CN–H_2O (50:50, v/v) to give **3** (27.7 mg) and **7** (41.5 mg), together with 280 mg untransformed **1**.

*4.3.1. Acacic acid lactone (**2**)*

Colorless needles; mp 240–242 °C; $[\alpha]_D^{24}$ 54.3 (*c* 0.08, MeOH); the asymmetric HPLC showed the purity was 96.4%; ^{1}H and ^{13}C NMR data were consistent with reported data.[20]

*4.3.2. 3β,16α-Dihydroxy-olean-11,13(18)-dien-28β-oic acid-21-lactone (**3**)*

White amorphous powder; mp 184–186 °C; $[\alpha]_D^{25}$ −39.8 (*c* 0.13, MeOH); IR (KBr) ν_{max} 3444, 2937, 1763, 1464, 1035, 993, 578 cm^{-1}; the asymmetric HPLC showed the purity was 95.4%; ^{1}H and ^{13}C NMR data were consistent with reported data [21].

*4.3.3. 3β,6β,16α-Trihydroxy-olean-12-en-28β-oic acid-21-lactone (**4**)*

White amorphous powder; mp 182–184 °C; $[\alpha]_D^{25}$ −40.9 (*c* 0.16, MeOH); IR (KBr) ν_{max} 3440, 2944, 2527, 1755, 1640, 1466, 1392, 1175, 1039, 621 cm^{-1}; the asymmetric HPLC showed the purity was 96.6%; ^{1}H and ^{13}C NMR data see Tables 1 and 2; HR-ESI-MS m/*z* 525.2981 (calcd for $C_{30}H_{46}O_5K$, 525.2977).

*4.3.4. 1β,3β,16α-Trihydroxy-olean-12-en-28β-oic acid-21-lactone (**5**)*

White amorphous powder; mp 198–199 °C; $[\alpha]_D^{25}$ −98.8 (*c* 0.23, MeOH); IR (KBr) ν_{max} 3462, 2951, 1766, 1467, 1042, 995, 619 cm^{-1}; the asymmetric HPLC showed the purity was 95.1%; ^{1}H and ^{13}C NMR data see Tables 1 and 2; HR-ESI-MS m/*z* 504.3691 $[M + NH_4]^+$ (calcd for $C_{30}H_{50}NO_5$, 504.3684).

*4.3.5. 3β,7β,16α-Trihydroxy-olean-12-en-28β-oic acid (**6**)*

White amorphous powder; mp 233–235 °C; $[\alpha]_D^{24}$ 118.2 (*c* 0.17, MeOH); IR (KBr) ν_{max} 3510, 3433, 2949, 1690, 1632, 1467, 1042, 984, 718 cm^{-1}; the asymmetric HPLC showed the purity was 97.8%; ^{1}H and ^{13}C NMR data see Tables 1 and 2; HR-ESI-MS m/*z* 489.3576 $[M + H]^+$ (calcd for $C_{30}H_{49}O_5$, 489.3575).

*4.3.6. 3β,7β,16α-Trihydroxy-olean-11,13(18)-dien-28β-oic acid (**7**)*

White amorphous powder; mp 185–187 °C; $[\alpha]_D^{24}$ −141.6 (*c* 0.28, MeOH); IR (KBr) ν_{max} 3440, 2942, 1701, 1463, 1042, 979, 721 cm^{-1}; the asymmetric HPLC showed the purity was 95.1%; ^{1}H and ^{13}C NMR data see Tables 1 and 2; HR-ESI-MS m/*z* 487.3419 $[M + H]^+$ (calcd for $C_{30}H_{47}O_5$, 487.3418).

4.4. Biotransformation of EA by A. alternata AS 3.4578

Different from the process by *R. chinensis* CICC 3043, mycelia of *A. alternata* AS 3.4578 from agar slants were aseptically transferred to 250 mL Erlenmeyer flasks containing 100 mL of liquid potato medium. The fungus was incubated at 25 °C on a rotary shaker (180 rpm) in the dark for 48 h to make a stock inoculum. Then 5 mL of the inoculum was added to each of the 1000 mL flasks containing 400 mL of potato medium. After 48 h incubation, a total amount of 900 mg of EA dissolved in 50 mL of EtOH was distributed equally among 50 flasks. The incubation was allowed to continue for seven additional days on the shaker. The cultures were then pooled and filtered through a filter paper. The filtrate was extracted with equal volume of EtOAc for three times. The EtOAc extract as a brown syrup was subjected to column chromatography, PR-18 and Sephadex LH-20, which was similar to that described above for the biotransformation of EA by *R. chinensis* CICC 3043, to give **5** (28.3 mg), **7** (5.6 mg), **8** (50.8 mg), **9** (18.2 mg), **10** (22.1 mg), **11** (63.1 mg), and **12** (132.6 mg), together with 200 mg untransformed EA.

*4.4.1. 1β,3β,16α-Trihydroxy-olean-12-en-28β-oic acid (**8**)*

White amorphous solid; mp 185–187 °C; $[\alpha]_D^{25}$ 179.6 (*c* 0.26, MeOH); IR (KBr) ν_{max} 3435, 2948, 1695, 1677, 1468, 1275, 998, 744 cm^{-1}; the asymmetric HPLC showed the purity was 95.7%; ^{1}H and ^{13}C NMR data see Tables 1 and 2; HR-ESI-MS m/*z* 489.3577 $[M + H]^+$ (calcd for $C_{30}H_{49}O_5$, 489.3575).

*4.4.2. 3β,16α,29-Trihydroxy-olean-12-en-28β-oic acid (**9**)*

White amorphous solid; mp 208–210 °C; $[\alpha]_D^{25}$ 156.0 (*c* 0.04, MeOH); IR (KBr) ν_{max} 3435, 2930, 2519, 1678, 1639, 1465, 1044, 999, 469 cm^{-1}; the asymmetric HPLC showed the purity was 95.5%; ^{1}H and ^{13}C NMR data see Tables 1 and 2, HR-ESI-MS m/*z* 489.3578 $[M + H]^+$ (calcd for $C_{30}H_{49}O_5$, 489.3575).

*4.4.3. 3-Oxo-16α-Hydroxy-olean-12-en-28β-oic acid (**10**)*

White amorphous solid; mp 230–233 °C; $[\alpha]_D^{24}$ 151.6 (*c* 0.14, MeOH); IR (KBr) ν_{max} 3524, 2949, 1719, 1679, 1449, 1224, 1004, 707 cm^{-1}; the asymmetric HPLC showed the purity was 98.1%; ^{1}H NMR, ^{13}C NMR and HRMS data were consistent with reported data.[22,23]

*4.4.4. 1β,3β,16α-Trihydroxy-olean-11,13(18)-dien-28β-oic acid (**11**)*

White amorphous solid; mp 188–190 °C; $[\alpha]_D^{25}$ −48.3 (*c* 0.06, MeOH); IR (KBr) ν_{max} 3433, 2923, 1636, 1457, 1060, 585, 457 cm^{-1}; the asymmetric HPLC showed the purity was 95.1%; ^{1}H and ^{13}C NMR data see Tables 1 and 2; HR-ESI-MS m/*z* 487.3412 $[M + H]^+$ (calcd for $C_{30}H_{47}O_5$, 487.3418).

*4.4.5. 3-Oxo-16α,29-Dihydroxy-olean-12-en-28β-oic acid (**12**)*

White amorphous solid; mp 200–202 °C; $[\alpha]_D^{24}$ 279.0 (*c* 0.65, MeOH); IR (KBr) ν_{max} 3455, 2932, 2866, 1699, 1461, 1386, 1044, 974, 534 cm^{-1}; the asymmetric HPLC showed the purity was 96.6%; ^{1}H and ^{13}C NMR data see Tables 1 and 2, HR-ESI-MS m/*z* 487.3409 $[M + H]^+$ (calcd for $C_{30}H_{47}O_5$, 487.3418).

*4.5. Alkaline hydrolysis of compound **2** (**13**)*

A sample of compound **2** (14.9 mg, 0.032 mmol) was saponified in 1% KOH/EtOH (5 mL) for 2.5 h at 60 °C. After neutralization with 0.5 N HCl/EtOH, the mixture was separated by silica gel chromatography to give compound **13** (12.9 mg, 84%) as white amorphous powder. mp 213–215 °C; the asymmetric HPLC showed the purity was 98.2%; ^{1}H NMR, ^{13}C NMR and HRMS data were consistent with reported data [35].

4.6. HCV and VSV pseudovirus entry assay

All compounds were tested using the HCV and VSV pseudo particle (HCVpp and VSVpp) entry assay as described previously [36,37].

4.7. Hemolytic assay

Hemolytic activity was measured as following [38]: 2% rabbit red blood cells (5×10^8 RBC/mL) in PBS buffer (pH 7.4) were incubated with serially diluted compounds. After incubating for 60 min at 37 °C, hemolysis was monitored by measuring absorption at 541 nm with a microplate reader. Percentage of hemolysis was then calculated by the routine method.

Acknowledgments

This work was supported by the National Basic Research Program of China (973 Program; grant no. 2010CB12300), the National Natural Science Foundation of China (grant nos. 20932001 20852001 and 81101239), Beijing Natural Science Foundation (grant no. 7102103), and Beijing NOVA Program (grant no. 2009B02).

Appendix A. Supplementary data

Supplementary data related to this article can be found at http://dx.doi.org/10.1016/j.ejmech.2013.03.041.

References

[1] X.A. Wen, H.B. Sun, J. Liu, K.G. Cheng, P. Zhang, L.Y. Zhang, J. Hao, L.Y. Zhang, P.Z. Ni, S.E. Zographos, D.D. Leonidas, K.M. Alexacou, T. Gimisis, J.M.H. ayes, N.G. Oikonomakos, Naturally occurring pentacyclic triterpenes as inhibitors of glycogen phosphorylase: synthesis, structure-activity relationships, and X-ray crystallographic studies, J. Med. Chem. 51 (2008) 3540–3554.

[2] Y. Allouche, F. Warleta, M. Campos, C. Sánchez-Quesada, M. Uceda, G. Beltrán, J.J. Gaforio, Antioxidant, antiproliferative, and pro-apoptotic capacities of pentacyclic triterpenes found in the skin of olives on MCF-7 Human Breast Cancer Cells and their effects on DNA damage, J. Agric. Food Chem. 59 (2011) 121–130.

[3] S. Alakurtti, T. Makela, S. Koskimies, K.J. Yli, Pharmacological properties of the ubiquitous natural product betulin, Eur. J. Pharm. Sci. 29 (2006) 1–13.

[4] M.O. Margaret, D.B. Michael, S.C. Christopher, J.W. Barbara, Betulin and lupeol in bark from four white-barked birches, Phytochemistry 27 (1998) 2175–2176.

[5] L.M. Pablos, G. González, R. Rodrigues, A.G. Granados, A. Parra, A. Osuna, Action of a pentacyclic triterpenoid, maslinic acid, against *Toxoplasma gondii*, J. Nat. Prod. 73 (2010) 831–834.

[6] L.G. Rocha, J.R.G.S. Almeida, R.O. Macêdo, J.M. Barbosa-Filho, A review of natural products with antileishmanial activity, Phytomedicine 12 (2005) 514–535.

[7] K.D. Qian, R.Y. Kuo, C.H. Chen, L. Huang, S.L. Morris-Natschke, K.H. Lee, Structure-activity relationship study of betulinic acid and moronic acid derivatives as potent HIV maturation inhibitors, J. Med. Chem. 53 (2010) 3133–3141.

[8] K.H. Lee, Discovery and development of natural product-derived chemotherapeutic agents based on a medicinal chemistry approach, J. Nat. Prod. 73 (2010) 500–516.

[9] A.D. Kinghorn, Natural product chemistry for drug discovery, J. Med. Chem. 53 (2010) 2329.

[10] D.L. Yu, Y. Sakurai, C.H. Chen, F.R. Chang, L. Huang, Y. Kashiwada, K.H. Lee, Anti-AIDS agents 69, moronic acid and other triterpene derivatives as novel potent anti-HIV agents, J. Med. Chem. 49 (2006) 5462–5469.

[11] L.J. Huang, W.Y. Gao, X. Li, W.S. Zhao, L.Q. Huang, C.X. Liu, Evaluation of the *in vivo* anti-inflammatory effects of extracts from *Pyrus bretschneideri* Rehd, J. Agric. Food Chem. 58 (2010) 8983–8987.

[12] T.H. Quang, N.T.T. Ngan, C.V. Minh, P.V. Kiem, N.X. Nhiem, B.H. Tai, N.P. Thao, N.H. Tung, S.B. Song, Y.H. Kim, Anti-inflammatory triterpenoid saponins from the stem bark of *Kalopanax pictus*, J. Nat. Prod. 74 (2011) 1908–1915.

[13] D.H. Kim, S.B. Shin, N.J. Kim, I.S. Jang, β-glucuronidase-inhibitory activity and hepatoprotective effect of *Ganoderma lucidum*, Biol. Pharm. Bull. 22 (1999) 162–164.

[14] G. Francis, Z. Kerem, H.P.S. Makkar, K. Becker, The biological action of saponins in animal systems: a review, Br. J. Nutr. 88 (2002) 587–605.

[15] R.B. Bacon, S.C. Gordon, E. Lawitz, P. Marcellin, J.M. Vierling, S. Zeuzem, F. Poordad, Z.D. Goodman, H.L. Sings, N. Boparai, M. Burroughs, C.A. Brass, J.K. Albrecht, R. Esteban, Boceprevir for previously treated chronic HCV genotype 1 infection, N. Engl. J. Med. 364 (2011) 1207–1217.

[16] M. Donald, M.D. Jensen, A new era of hepatitis C therapy begins, N. Engl. J. Med. 364 (2011) 1272–1274.

[17] M. Ye, G.Q. Qu, H.Z. Guo, D.A. Guo, Novel cytotoxic bufadienolides derived from bufalin by microbial hydroxylation and their structure–activity relationships, J. Steroid. Biochem. 91 (2004) 87–98.

[18] M. Ye, G.Q. Qu, H.Z. Guo, D.A. Guo, Specific 12β-hydroxylation of cinobufagin by filamentous fungi, Appl. Environ. Microbiol. 70 (2004) 3521–3527.

[19] A. Dong, M. Ye, H.Z. Guo, J.H. Zheng, D.A. Guo, Microbial transformation of ginsenoside Rb1 by *Rhizopus stolonifer* and *Curvularia lunata*, Biotechnol. Lett. 25 (2003) 339–344.

[20] M.A. Gafur, T. Obata, F. Kiuchi, Y. Tsuda, Chemical constituents of the flora of Jordan, Chem. Pharm. Bull. 45 (1997) 620–625.

[21] G.M. Rukunga, P.G. Waterman, Triterpenes of *Albizia versicolor* and *Albizia schimperana* stem barks, Fitoterapia 72 (2001) 188–190.

[22] L.V. Alegrio, G. Massiot, C. Lavaud, L. Le Men-Olivier, T. Sevenet, Terpene esters from *Archidendropsis streptocarpa* (Fournier) Nielsen, Plantes médicinales et phytothérapie 26 (1993) 101–108.

[23] X. Feng, Z.M. Zou, S.B. Fu, L.Z. Sun, Z.H. Su, D.A. Sun, Microbial oxidation and glucosidation of echinocystic acid by *Nocardia coralline*, J. Mol. Catal. B-enzym 66 (2010) 219–223.

[24] S.P. Bai, L. Dong, Z.A. He, L. Yang, A new triterpenoid from *Doellingeria scaber*, Chin. Chem. Lett. 15 (2004) 1303–1305.

[25] F.Y.Q. Wang, Z. Zhang, Y.Y. Peng, Y.Y. Shi, Y.X. Zheng, S.L. Xiao, H. Wang, Y.Y. Qiu, X.X. Huang, C.K. Zhao, C.L. Zhang, D.A. Sun, L.H. Zhang, D. M. Zhou (unpublished work).

[26] X.W. Yu, L.L. Wang, Y. Xu, *Rhizopus chinensis* lipase: gene cloning, expression in *Pichia pastoris* and properties, J. Mol. Catal. B-enzym 57 (2009) 304–311.

[27] K. Takao, S. Tokunosuke, K.K. Takeatsu, Studies on the constituents of leguminous plants. The structure of triterpenoid saponins from fruits of *Gymnocladus chinensis* baillon, Chem. Pharm. Bull. 32 (1984) 4833–4841.

[28] K. Junei, A. Kaoru, F. Katsura, H. Hiroyuki, I. Tuyoshi, N. Toshihiro, I. Yoshiteru, T. Norimichi, M. Masazumi, S. Junzo, Six new triterpenoidal glycosides including two new sapogenols from *Albizziae* cortex, Chem. Pharm. Bull. 12 (1992) 3269–3273.

[29] H.Y. Young, S.W. Won, S.C. Jae, S.K. Sam, Isolation of a new sapogenin from *Albizzia julibrissin*, Arch. Pharmacal. Res. 5 (1982) 33–38.

[30] C. Gauthier, J. Legault, S. Lavoie, S. Rondeau, S. Tremblay, A. Pichette, Synthesis and cytotoxicity of bidesmosidic betulin and betulinic acid saponins, J. Nat. Prod. 72 (2009) 72–81.

[31] A.A. Magid, L. Voutquenne, C. Moretti, C. Long, C. Lavaud, Triterpenoid Saponins from the fruits of *Caryocar glabrum*, J. Nat. Prod. 69 (2006) 196–205.

[32] Z.T. Wang, S.J. Wang, F. Zhu, Z.X. Chen, L.S. Yu, S. Zeng, Determination of enantiomeric impurity in besifloxacin hydrochloride by chiral high-performance liquid chromatography with precolumn derivatization, Chirality 24 (2012) 526–531.

[33] S. Hideo, Y.F. Norio, T. Tomonori, U. Tsukasa, Chiral assay of omeprazole and metabolites and its application to a pharmacokinetics related to CYP2C19 genotypes, J. Chromatogr. B. 879 (2011) 2465–2470.

[34] N. Ullah, W. Seebacher, R. Weis, J. Jurenitsch, K. Rauchensteiner, E. Haslinger, Synthesis and hemolytic properties of glycyrrhetic acid glycosides, Monatshefte für Chem. 131 (2000) 787–794.

[35] M. Hsu, J. Zhang, M. Flint, C. Logvinoff, C. Cheng-Mayer, C.M. Rice, J.A. McKeating, Hepatitis C virus glycoproteins mediate pH-dependent cell entry of pseudotyped retroviral particles, Proc. Natl. Acad. Sci. 100 (2003) 7271–7276.

[36] J.P. Yang, D.M. Zhou, F. Wong-Staal, Screening of small-molecule compounds as inhibitors of HCV entry, Methods Mol. Biol. (2009) 295–304. second ed.

[37] B. Bartosch, J. Dubuisson, F.L. Cosset, Infectious hepatitis C virus pseudo-particles containing functional E1–E2 envelope protein complexes, J. Exp. Med. 197 (2003) 633–642.

[38] G.X. Luo, R. Colonno, M. Kyrstal, Characterization of a hemagglutinin-specific inhibitor of influenza A virus, Virology 226 (1996) 66–76.